Annals of Glaciology 37 2003
© International Glaciological Society

Snow-accumulation studies in Antarctica with ground-penetrating radar using 50, 100 and 800 MHz antenna frequencies

ANNA SINISALO,[1] ASLAK GRINSTED,[1] JOHN C. MOORE,[1] EIJA KÄRKÄS,[2] RICKARD PETTERSSON[3]

[1]*Arctic Centre, University of Lapland, Box 122, FIN-96101 Rovaniemi, Finland*
E-mail: anna.sinisalo@urova.fi
[2]*Division of Geophysics, Department of Physical Sciences, P.O. Box 64, University of Helsinki, FIN-00014 Helsinki, Finland*
[3]*Department of Physical Geography, Stockholm University, S-106 91 Stockholm, Sweden*

ABSTRACT. Snow radar profiles were measured in Dronning Maud Land, East Antarctica, in the vicinity of the Finnish research station Aboa during austral summer 1999/2000. The aim was to study the annual layering in the upper 50 m of the snowpack and to compare the results obtained by three radar antenna frequencies (50, 100 and 800 MHz). Intercomparison of the radar profiles measured by the three frequencies shows that some individual internal layers are visible with different antennas. Sparse accumulation-rate data from stake measurements and snow pits are compared with layer depths. The comparison reveals a great deal of scatter due to the large interannual variability in accumulation patterns. Using the radar layers as isochrones together with a model of depth–density–radar-wave velocity allows the individual accumulation data to be integrated, and a better estimate of accumulation patterns is obtained. Using the radar layering seems to be a much better method of estimating accumulation rate in this region than using a short series of stake measurements, even in the absence of deep ice cores to directly date the radar layering.

INTRODUCTION

The mass balance of Antarctica is insufficiently well known. More data are desirable in the context of current and possible future changes in climate, and the concomitant response of the Antarctic ice sheet. Significant progress has been made using various remote-sensing methods including ground-based and satellite radar sounding, but a major source of uncertainty is the probable large variability in accumulation and possibly snow properties both spatially and temporally, especially in regions close to the coast and in mountainous terrain. Accurate snow-accumulation data over these regions are required in order to obtain a reliable mass-balance estimate. Ground-penetrating radar (GPR) has been successfully used for snow-accumulation studies in Svalbard (Kohler and others, 1997; Pälli and others, 2002) and Antarctica (Richardson and others, 1997). The advantage of using GPR is that it is time-efficient; large areas can be covered quickly and the temporal and spatial variability in snow accumulation obtained. The disadvantage is that for the accumulation rates to be absolute rather than relative, the radar layers must be dated in at least one location (usually with an ice core). Once the depth–density profile is accounted for, and any layer thinning due to ice flow corrected for, the present and past accumulation rates can be found (e.g. Morse and others, 1998; Pälli and others, 2002). As we lack an ice core along our radar profile, we use the limited accumulation-rate data from a few stakes and pits along the profile to estimate the age of radar layers.

Snow-accumulation studies usually employ high-frequency radars because of their their high resolution (Richardson and others, 1997), but low-frequency radars (e.g. 50 MHz) can also be effective (Pälli and others, 2002). The lower frequencies are particularly useful for determining the accumulation rates further in the past or over longer time periods, as they have much greater penetration depths and tend to show only the strongest, most continuous reflectors. Few studies however, have been based on the results obtained using different radar antenna frequencies. Fujita and others (1999) compare pulse radar frequencies of 60 and 179 MHz within the topmost 100–700 m of the surface of the East Antarctic ice sheet, and discuss the various scattering mechanisms. In this paper, we compare three different antenna frequencies for accumulation studies within the uppermost 50 m of the snowpack in Antarctica. We used a commercial Ramac GPR (Malå Geoscience).

FIELD DATA

A 5.5 km stake line (see Fig. 1) was measured with antenna frequencies of 50, 100 and 800 MHz in order to compare the reflection horizons and study the cause of the reflections. The line started on the glacier about 6 km from the Finnish research station Aboa. The first 5 km are on level terrain, while the last 500 m ascend the slope of the Basen nunatak to Aboa. The bedrock drops quickly away from Basen to give an ice thickness of 300–400 m along the profile (Ruotoistenmäki and Lehtimäki, 1997). Two snow pits and a 10 m core (A2) were drilled along this profile (Fig 1). Snow-accumulation-rate data for 2 years are available from several stakes along the line, and from several earlier sets of stake measurements along the profile, which has been on the area's main route southward for many years.

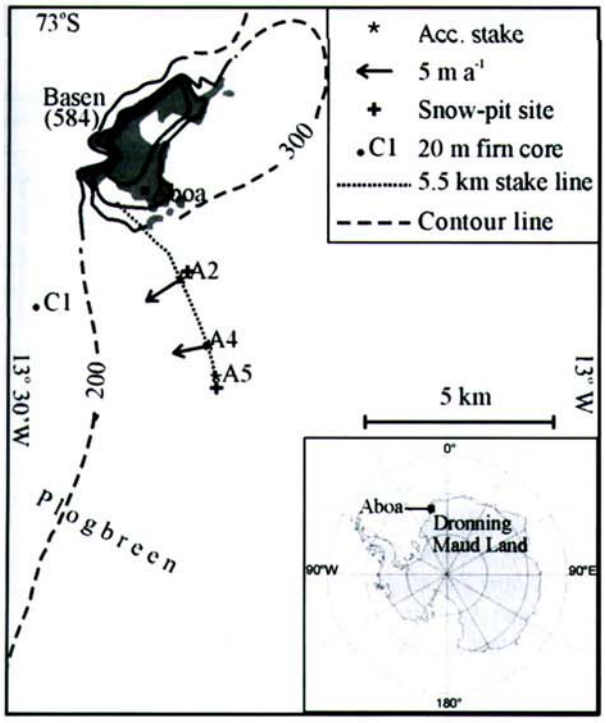

Fig. 1. Map of the Aboa area showing the radar transect and the location of the cores, snow pits, stakes and surface velocity vectors (arrows) for the A2 and A4 stakes.

The radar technique involved driving the profile lines on a snowmobile carrying a differential global positioning system (GPS) (Javad Positioning System). The radar transmitter and receiver antennas for the 50 MHz measurements were mounted on a non-metallic sledge, which was pulled 7 m behind the snowmobile. The radar control unit and computer were mounted on the snowmobile together with the roving GPS receiver. The 800 and 100 MHz antennas were shielded units and could be pulled closer behind the snowmobile: the 100 MHz system was pulled about 5 m behind in its own sealed housing; the 800 MHz system was pulled about 2 m behind the snowmobile using rigid struts to keep it at a fixed distance. No trace stacking was done, and data were collected on a laptop computer. Table 1 shows the radar collection parameters. Post-processing of the radar data was done using the Haescan program (Roadscanners Oy). Amplitude zero-level correction was applied, background noise was removed and vertical high-pass and low-pass filtering in time domain was performed.

We compare our radar accumulation-rate data with those derived from snow-pit and core observations along the profile. The cores and the snow pits were sampled to delineate

Table 1. Measurement parameters for each antenna in the GPR survey

Antenna frequency	*Number of samples*	*Time window*	*Trace interval*	*Average trace interval*
MHz		μs	s	m
50	2048	4.762	0.5	1.7
100	2048	2.286	0.5	1.7
800	1024	1.968	0.25	0.8

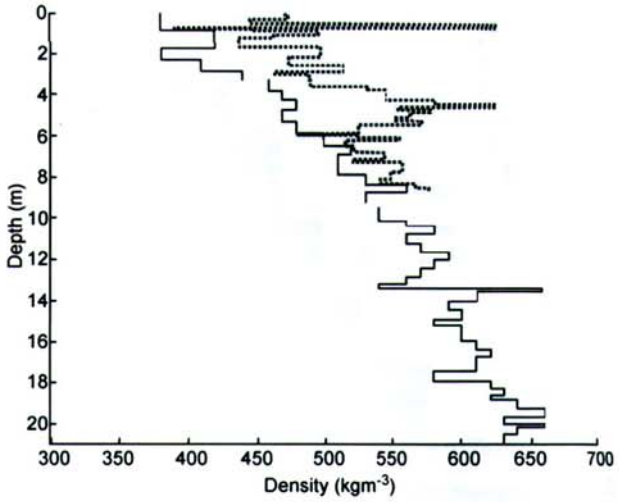

Fig. 2. Density profiles from the 20 m C1 (solid line) and 10 m A2 (dashed line) cores.

stratigraphy and density. Figure 2 shows the density profiles obtained from the A2 core and the 20 m C1 core obtained a few km to the west of the profile.

COMPARISON OF ANTENNA FREQUENCIES

Vertical resolution in firn of the 800, 100 and 50 MHz antennas estimated from their bandwidths is about 0.2, 1.4 and 2.5 m, respectively. Thus, the radar response measured with the lower frequencies does not originate from individual layers, but more likely it results from many reflectors as interference patterns (Moore, 1988; Kohler and others, 1997). For the two lower antenna frequencies, the data show no response from the upper 1–2 m due to the length of the transmitted pulse.

Figure 3 shows the radar stratigraphy for the three frequencies along the profile line. To compare the various reflections seen at the different frequencies, we picked the strongest, most continuous reflecting horizons that are visible in more than one profile with different antenna frequencies. The amplitude of the reflections varies from place to place, but we chose the layers that are generally visible throughout the profile. The large range in antenna properties means that only a few layers overlap, and we have picked out two layers that appear on more than one radar profile. We also marked layers 1 and 4, which are only visible in the 800 and 50 MHz data, respectively, to indicate the range of layering available with the different antennas. There are no single continuous reflecting horizons in the 800 MHz profile, but what appear more like reflection bands. The high resolution of the antenna and the relatively long horizontal trace interval (about 0.8 m) probably explains this. The high resolution allows scattering from very thin, discontinuous and weakly reflecting layers to be observed, confusing the general picture. Many strong, continuous layers are visible in the 100 and 50 MHz profiles (Fig. 3).

The subsurface undulation of the radar horizons is consistent in all the GPR profiles. It is widely accepted that the radar layers are isochrones (e.g. Richardson and others, 1997; Morse and others, 1998; Fujita and others, 1999) and that their depth is therefore related to accumulation rates and also to the ice flow. The surface ice-flow velocity is almost perpendicular to the profile (Fig. 1), but at 5 m a^{-1}, even ice that is 100 years old and 50 m deep will have origi-

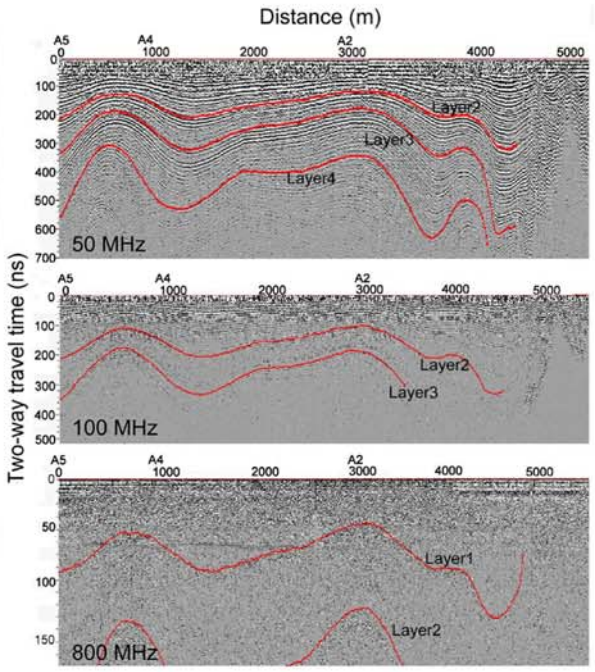

Fig. 3. The complete radar profiles at (top to bottom) 50, 100 and 800 MHz along the 5.5 km profile. Layers 1–4 are marked in the profiles, and ages are modelled at sites A5, A4 and A2 (Table 2).

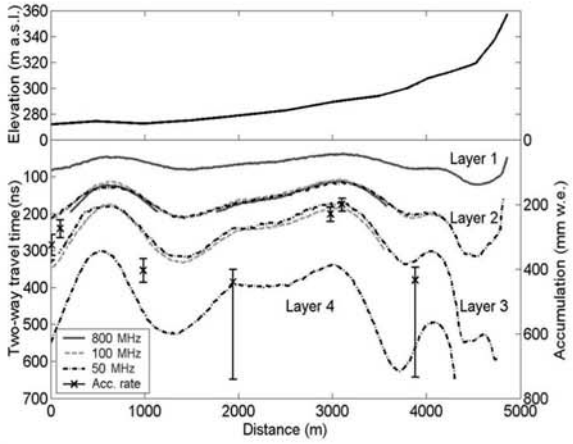

Fig. 4. Four layers seen in the radar profiles (Fig. 3): 800 MHz data shown as solid lines in dark grey, 100 MHz data as dashed lines in light grey, and 50 MHz data as dash-dot lines in black. Layer 1 (top) is seen only in 800 MHz data; layer 2 in all data; layer 3 in 50 and 100 MHz data; and layer 4 only in 50 MHz data. The accumulation rates derived from the snow pits and stake measurements are shown as black squares with the error bars. Surface topography along the profile is shown at the top.

nated only about 500 m away from the profile. The undulations of the radar horizons are clearly related to the surface topography along the profile (Fig. 4). There is a small surface hump at about 600–700 m along the profile. Figure 4 shows that the layers are shallowest near the top of this surface hump, though the exact horizontal position of this feature relative to the surface rise is to the north in the radar layers close to the surface and to the south in the deeper layers. The surface elevation is lowest in the beginning of the profile (southern end), and there is another surface trough at 1000 m (Fig. 4). The local layer depth maximum is 200–400 m north of the surface trough, and the depth maximum is further south in deeper layers. The horizontal displacement of the layer depth maximum shows more variation than the layer depth minimum at the surface hump. Ruotoistenmäki and Lehtimäki (1997) provide a map of bedrock topography along the profile, showing a local rise that is about 100 m higher than the bedrock elevation within 1 km on each side of it. This bedrock rise is in the vicinity of the observed surface hump, and must control the surface topography despite local accumulation-rate effects acting to smooth the topography.

ACCUMULATION RATES

Accumulation rates along the line are available from two sources. Detailed snow-pit stratigraphy gives accumulation rates at 0.1 and 3.1 km distance (Fig. 4), and from repeat measurements of stake exposure above the snow surface. We use density data from the two pits (at A5 and A2) to estimate water equivalent accumulation. Of five stakes originally placed along the 5 km section of line in January 1997 (personal communication from T. Ruotoistenmäki, 2000), two were not found (presumably they were buried, though they may have been blown away), so we have stake accumulation data spanning 2 years at three sites A5, A4 and A2 (at 0, 0.98 and 2.98 km distance). The buried stakes also give minimum accumulation rates; we assume that 20 cm of the stakes were above the snow surface but could not be seen (data at 1.94 and 3.88 km; Fig. 4).

It can be seen in Figure 4 that the accumulation rates follow the general pattern of highs and lows in the radar layering. However, a direct comparison requires conversion of the radar layering to a real snow depth and then to an age to verify that the layer is at a depth consistent with accumulation rates and density structure at the particular place along the profile. We can neglect the differential layer thinning due to ice flow, as we are concentrating on the top 50 m of the 300–400 m thick ice sheet. To compare how well the accumulation rates measured from the stakes agree with the radar isochrones, we must model the densification rate and age–depth and radar-travel-time–depth relations at locations along the traverse. We do this using the densification model of Herron and Langway (1980) which requires knowledge of surface density, accumulation rate and 10 m temperature. We have good data to do this at 0 km, where we have stake accumulation rates and densities from a snow pit, and at site A2 where we also have stake accumulation rates, the ice 10 m temperature from the borehole (−17°C) and density. Site A4 (0.98 km) also has good accumulation-rate information, and we assume densities averaged between snow pits. With the Herron and Langway (1980) densification model, the radar two-way travel time t to any layer depth can then be calculated from the empirical equation (Robin, 1975)

$$t = \frac{1}{c}\left\{\left[(1 + 0.85\rho)\sqrt{l_a^2 + 4D^2}\right] - l_a\right\}, \qquad (1)$$

where c is the speed of light, ρ is the average snow density (relative to water) between the surface and a depth D, and l_a is the antenna separation (15 cm for the 800 MHz, 1 m for the 100 MHz and 2 m for the 50 MHz system). We neglect wave refraction within the snowpack since density changes

Table 2. Model ages (years) of four layers at sites A2, A4 and A5

Location (distance in km in Fig. 3)	Layer 1	Layer 2	Layer 3	Layer 4
A5 (0)	15	42–43	69–73	120
A4 (0.98)	8	25–27	39–42	79
A2 (2.98)	9	29–31	47–50	97

Notes: Parameters used in the model: 10 m temperature = −17°C; A5: b = 0.325 m a^{-1}, $\rho_{surface}$ = 464 kg m^{-3}; A4: b = 0.404 m a^{-1}, $\rho_{surface}$ = 435 kg m^{-3}; A2: b = 0.23 m a^{-1}, $\rho_{surface}$ = 402 kg m^{-3}.

Layer1: 800 MHz only; layer 2: all antennas except no 800 MHz data at A5; layer 3: 50 and 100 MHz antennas; layer 4: 50 MHz only.

have a negligible effect on wave path length with such small antenna separations.

Table 2 compares the model ages of the four prominent layers seen in Figures 3 and 4 by each antenna at three locations. There is clearly a lot of scatter in the ages derived for the layer. It may be that the radar layering is not an isochrone, possibly because of interference effects. However, the sensitivity to interference effects can be estimated by comparing the ages of layers with the different antennas, which is the range shown in each cell for layers 2 and 3 in Table 2 and is no more than a few years. The degree of scatter in the modeled ages is therefore largely due to the sensitivity of the model to the accumulation rate at each site, which is affected by the rather large interannual variability of precipitation and the snow density. Figure 2 shows that the density profiles of cores in the region can differ in the upper few metres, and the pit at A5 has a near-surface density of 464 kg m^{-3} compared with that at A2 of 402 kg m^{-3}. Isaksson and Karlén (1994) report the 1988 and 1989 accumulation rates along an earlier stake line on the same route with about a 50% lower accumulation in 1988 than in 1989. A firn core from about 30 km south of the profile spanning the years 1975–89 showed similar interannual variations and a net decrease from about 45 to 25 cm w.e. a^{-1} over the whole time period (Isaksson and Karlén, 1994). However, Sommer and others (2000) report that decadal variability of 20% in accumulation is typical of Dronning Maud Land, and Richardson and others (1997), on the basis of radar estimates of snow layering, conclude that the area exhibits generally static accumulation patterns with large year-to-year variations, probably due to variations in wind variability accentuated by the local nunataks. These results highlight the errors possible in estimating accumulation rates from very short series of measurements on stakes and on density data from a small number of snow pits.

We may assume that accumulation rates have not changed significantly over the past 100 years at any particular place along the radar profile, and therefore the best age estimate of the layers in Table 2 is the mean of the ages at each site. This procedure allows all the accumulation data to be utilized in a consistent way to derive a set of ages. From the layer ages, the accumulation is then immediately available along the profile, using the densification model with Equation (1). Using this procedure, the long-term accumulation rate at A5 is rather more than that found from the pit and stake measurements from the last 2 years. If the surface snow density were closer to that at A2 (or indeed to the other pits and ice-core sites in the area, such as C1), then the modeled layer ages would be about 15% less, putting them very close to the A2 estimates.

It is clear that the accumulation-rate data given by each antenna are equally valid, so the difference between the antennas is about the trade-off between resolution and depth of penetration, as all seem adept at following layering that can give accumulation rates. Potentially the 800 MHz radar should reveal individual annual layers, but the variation in layer thickness along the profile in this mountainous region would require more closely spaced traces than are used here.

CONCLUSIONS

Comparison of radar profiles obtained at three different frequencies along a 5.5 km route highlights the complementary layering seen at each frequency. From the practical viewpoint of studying snow accumulation, the higher frequency (800 MHz) obviously gives the best resolution, especially in the upper few metres. However, the scattering of the radar energy from many individual points makes the snow layering harder to follow with the high-frequency antenna. Probably the performance would have been better with a shorter horizontal trace interval. The 50 and 100 MHz profiles give much clearer layering, as they tend to smooth local variations in the snowpack, at the expense of lower vertical resolution, and loss of signal in the upper metres. However, the layering at all frequencies is consistent in terms of its variability along the profile, and seems to be correlated with surface topography (reflecting bed topography) and with accumulation found from snow pits and stake measurements.

Using depth–density and depth–radar-travel-time relations, the age of radar layers can be estimated based on surface estimates of accumulation rate and temperature. We find that this gives ages with rather large scatter for continuous radar layers, which are known to be isochrones. However, the scatter is much more likely to be due to errors in the mass-balance data than to errors in radar interpretation caused by interference effects or lack of resolution. Once the age of a radar layer is determined, the accumulation rate follows from the depth–density–travel-time model used. The radar accumulation measurements have the advantage over traditional stake mass-balance measurements that they can be used to integrate the separate short time series from stake data into more reliable mass-balance measurements by utilizing the fact that the radar layers are isochrones.

ACKNOWLEDGEMENTS

We are grateful to J. Vehviläinen for his help in the field and for providing some of the density data. The 1999/2000 field logistics were provided by the Finnish Antarctic Research Programme (FINNARP) 2000. The work is funded by the Finnish Academy and the Thule Institute. Some GPS data were kindly supplied by E. Asenjo and I. Andersson of the Swedish Antarctic Research Programme (SWEDARP), and T. Ruotoistenmäki provided original stake data. We thank two anonymous reviewers for helpful comments.

REFERENCES

Fujita, S. *and 6 others*. 1999. Nature of radio-echo layering in the Antarctic ice sheet detected by a two-frequency experiment. *J. Geophys. Res.*, **104**(B6), 13,013–13,024.

Herron, M. M. and C. C. Langway, Jr. 1980. Firn densification: an empirical model. *J. Glaciol.*, **25**(93), 373–385.

Isaksson, E. and W. Karlén. 1994. Spatial and temporal patterns in snow

accumulation, western Dronning Maud Land, Antarctica. *J. Glaciol.*, **40**(135), 399–409.

Kohler, J., J. Moore, M. Kennett, R. Engeset and H. Elvehøy. 1997. Using ground-penetrating radar to image previous years' summer surfaces for mass-balance measurements. *Ann. Glaciol.*, **24**, 355–360.

Moore, J. C. 1988. Dielectric variability of a 130 m Antarctic ice core: implications for radar sounding. *Ann. Glaciol.*, **11**, 95–99.

Morse, D. L., E. D. Waddington and E. J. Steig. 1998. Ice age storm trajectories inferred from radar stratigraphy at Taylor Dome, Antarctica. *Geophys. Res. Lett.*, **25**(17), 3383–3386.

Pälli, A. *and 6 others*. 2002. Spatial and temporal variability of snow accumulation using ground-penetrating radar and ice cores on a Svalbard glacier. *J. Glaciol.*, **48**(162), 417–424.

Richardson, C., E. Aarholt, S.-E. Hamran, P. Holmlund and E. Isaksson 1997. Spatial distribution of snow in western Dronning Maud Land, East Antarctica, mapped by a ground-based snow radar. *J. Geophys. Res.*, **102**(B9), 20,343–20,353.

Robin, G. de Q. 1975. Velocity of radio waves in ice by means of a bore-hole interferometric technique. *J. Glaciol.*, **15**(73), 151–159.

Ruotoistenmäki, T. and J. Lehtimäki. 1997. Estimation of permafrost thickness using ground geophysical measurements, and its usage for defining vertical temperature variations in continental ice and underlying bedrock. *J. Glaciol.*, **43**(144), 359–364.

Sommer, S. *and 9 others*. 2000. Glacio-chemical study spanning the past 2 kyr on three ice cores from Dronning Maud Land, Antarctica. 1. Annually resolved accumulation rates. *J. Geophys. Res.*, **105**(D24), 29,411–29,421.